Astrophysics and Space Science (2023) 368:80
https://doi.org/10.1007/s10509-023-04236-9

RESEARCH

Statistical determination of the distance to the Galactic Centre and the outset of the Milky Way old bulge: astrophysical conclusions

Evgeny Griv[1] · Ing-Guey Jiang[2,3] · Daniel Majaess[4,5] · Dante Minniti[5,6,7]

Received: 16 June 2023 / Accepted: 14 September 2023 / Published online: 29 September 2023

Abstract
In this concluding work of the series, a sample of selected $\sim 20{,}000$ type-ab RR Lyrae stars from a total of 39,617 sources of the old bulge at distances $r < 3.5$ kpc from the Galactic Centre (GC) identified in the Vista Variables in the Vía Láctea survey (VVV) via the latest sample of the VIrac VAriable Classification Ensemble (VIVACE) pipeline is leveraged. As a model of the bulge, an oblate spheroid of stars with two major perpendicular axes a and b situated in the Galactic plane and a minor axis c perpendicular to this plane is adopted. The spatial distribution of stars is approximated by a standard power law with constant flattening and truncations at the lower and upper limits while allowing for the Sun's distance from the GC r_0, the power-law index α, and the oblateness $q = c/a$ to be free parameters. Our estimate of the distance is $r_0 = 8.15 \pm 0.04$ kpc. The implied r_0 is almost the same for $1.5 < r_{\max} < 3.5$ kpc, while the $|\alpha|$ and q values are varying systematically with increasing truncation radius $r_{\max}$ in the ranges $1.56 - 2.66$ and $1.0 - 0.76$. A weighted average and weighted uncertainty associated with all our measurements of r_0 in the series is also taken, $r_0 = 8.2 \pm 0.1$ kpc. We argue that the ensuing result may be among the most robust indirect estimates that exist, as certain of the findings are tied to passbands of the Optical Gravitational Lensing Experiment (OGLE) RR Lyraes and globular clusters, and to near-infrared passbands of the VVV Type II Cepheids and VIVACE-VVV RR Lyraes. The distribution of stars within ≈ 3 kpc from the GC is spherical-like, $q \approx 1$. The average power-law indexes derived from the distribution of bulge RRab and inner halo globular clusters are nearly identical. This pertinent result demonstrates that the old bulge and inner halo form a continuous subsystem, and the bulk of the bulge objects represents the inner extension of a centrally concentrated, almost axisymmetric halo in the Galaxy.

Keywords Galaxy: fundamental parameters · Galaxy: kinematics and dynamics · Galactic bulge · Galactic halo · Galaxy: structure

1 Introduction

Accurately measuring the distance between the Sun and the Galactic Centre (GC) r_0 is important for defining all kinematic distances in the Milky Way and most estimates of the gravitational and luminous mass of both the system and objects within the system as well as extragalactic distances (e.g. Genzel et al. 2010). In reality, the exact value of r_0 is still not certain (e.g. Leung et al. 2023), although Bland-Hawthorn and Gerhard (2016) have obtained an overall best estimate of the Sun's distance from independent determinations of r_0 available to the end of 2015

$$r_0 = 8.2 \pm 0.1 \text{ kpc}.$$

Such a value of r_0 was obtained by computing the standard error of the weighted mean and the unbiassed standard error of the weighted mean of measurements for various samples of objects and then considering possible correlations

✉ E. Griv
griv@bgu.ac.il

1 Department of Physics, Ben-Gurion University of the Negev, Beer-Sheva 8410501, Israel

2 Department of Physics and Institute of Astronomy, National Tsing-Hua University, Hsin-Chu 30013, Taiwan

3 Center for Informatics and Computation in Astronomy, National Tsing-Hua University, Hsin-Chu 30013, Taiwan

4 Department of Chemistry and Physics, Mount Saint Vincent University, Halifax, Nova Scotia, B3M 2J6 Canada

5 Departamento de Fisica, Universidade Federal de Santa Catarina, Trinidade 88040-900, Florianópolis, Brazil

6 Departamento de Ciencias Físicas, Universidad Andres Bello, Fernández Concha 700, Las Condes, Santiago, Chile

7 Vatican Observatory, V00120 Vatican City State, Italy

between some of the measurements. Camarillo et al. (2018) have provided a value of

$$r_0 = 8.0 \pm 0.3 \text{ kpc}$$

(2σ error) by compiling 28 independent measurements available to the end of 2018. Exploiting Very Long Baseline Interferometry (VLBI) unprecedented accurate parallaxes with accuracies typically about ± 0.02 μas (e.g. Reid 2022), Reid et al. (2019) obtained

$$r_0 = 8.15 \pm 0.15 \text{ kpc}$$

by modeling the space motions of approximately 200 molecular masers associated with very young high-mass stars. Do et al. (2019) and GRAVITY Collaboration (2019) derived

$$r_0 = 7.946 \pm 0.050 \text{ (stat. error)} \pm 0.032 \text{ (syst. error) kpc}$$

and

$$r_0 = 8.178 \pm 0.013 \text{ (stat. error)} \pm 0.022 \text{ (syst. error) kpc},$$

respectively, using direct long-spanning for more than two decades measurements of the motion of the S2 star orbiting the Milky Way's supermassive $\approx 4 \times 10^6 M_\odot$ black hole Sgr A*, which is expected to be very close to being at rest in the GC (Genzel et al. 2010).[1] Removal of optical aberrations effect in GRAVITY Collaboration measurements brings the estimate of the Sun's distance of

$$r_0 = 8.275 \pm 0.091 \text{ (stat. error)} \pm 0.033 \text{ (syst. error) kpc}$$

(GRAVITY Collaboration 2021). Especially notice the $\sim 5\sigma$ disagreement between Do et al. (2019) and GRAVITY Collaboration (2021) estimates. The VLBI Exploration of Radio Astrometry Collaboration (VERA Collaboration 2020) direct measurements of trigonometric annual parallaxes of 99 strong maser sources distributed across the Galaxy yielded

$$r_0 = 7.920 \pm 0.160 \text{ (stat. error)} \pm 0.300 \text{ (syst. error) kpc}.$$

(There are many different methods to measure r_0, which may be divided into direct and indirect ones. See Genzel et al. (2010) and Bland-Hawthorn and Gerhard (2016) for an explanation of the difference between direct and indirect estimates of r_0.) Iwanek et al. (2023) determined the distance to the GC

$$r_0 = 7.66 \pm 0.01 \text{ (stat. error)} \pm 0.39 \text{ (syst. error) kpc},$$

examining the spatial distribution of 65,981 Mira variable stars discovered by the Optical Gravitational Lensing Experiment (OGLE) survey. Leung et al. (2023) estimated the Sun's distance using the kinematics of stars in the Galactic bar region derived from APOGEE DR17 and *Gaia* EDR3 data supplemented with spectrophotometric distances from the *astroNN* neural-network method,

$$r_0 = 8.23 \pm 0.12 \text{ kpc}.$$

Next, the old Galactic bulge origin, size, and orientation parameters are also still being disputed. We support a model of a 'classical bulge' that looks almost identical to slowly rotating, pressure-supported elliptical galaxies (Dékány et al. 2013; Kormendy 2016), populated by $\gtrsim 10$ Gyr old objects deficient in the heavy elements (Valenti et al. 2016; Simion et al. 2017). The bulge is roughly 5 to 7 kpc in diameter and contains a small part of the visible mass of the system (Gonzalez and Gadotti 2016; Navarro et al. 2021). This is the exact opposite of the so-called 'boxy and X-shaped bulge' (or 'disk pseudobulge') which is very probably formed from the Galactic thin disk via dynamical instabilities during the slow ('secular') evolution of the system (Saito et al. 2011; Kormendy 2016; Ness and Lang 2016; Semczuk et al. 2022; Iwanek et al. 2023). In particular, spiral-driven instabilities may drive gas inflow to enhance central star formation leading to secular growth of pseudobulges in rapidly rotating, rotationally-supported galactic disks (Yu et al. 2022). The principal conclusion derived from the aforementioned efforts is that the old bulge and inner halo may form a continuous subsystem, and the bulk of the bulge objects may represent the inner extension of a centrally concentrated and almost axisymmetric halo (see Griv et al. 2021, and discussion therein).[2]

RR Lyrae stars are excellent tracers of the oldest stellar populations and standard candles to measure the distance to stellar systems composed prevalently by an ancient, metal-poor stellar population that plays a crucial role in several astrophysical circumstances. The small scatter in RR Lyraes mean absolute magnitudes make them rather accurate distance indicators with which distances can be determined at a $\pm 5\%$ level precision or even better (e.g. Medina et al. 2023). Generally, these variable, low-mass, giant A2-F6 type, and kinematically hot stars do not trace a strong bar-like structure in the direction of the bulge at Galactocentric distances $r < 3$ kpc. This is likely because the triaxial perturbing potential field of the bar only weakly affects an older population with high random (turbulent) velocities (Alcock et al. 1998; Dékány et al. 2013; Kunder et al. 2016; Griv et al.

[1] Do et al. (2019) and GRAVITY Collaboration (2019) exploited the exact same object, although with different data sets. The two groups also differ in the astrometric reference system they employ.

[2] The chemical and kinematic as well as density distribution results suggest that the Galactic halo has two distinct components, particularly, the inner halo and outer halo, with a break radius of ≈ 30 kpc (e.g. Liu et al. 2021).

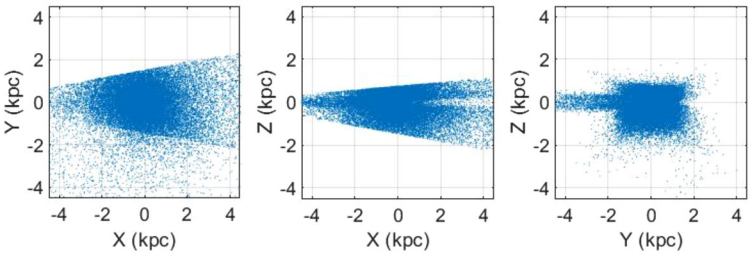

Fig. 1 Spatial distribution of all $N_{\rm total} = 39{,}617$ RRab used in this work in a Cartesian (X, Y, Z) coordinate system centered on the GC, with the Sun at $(-8.15, 0, 0.015)$ kpc

2020). Age-old stars do not trace a strong bar but obey a rather spheroidal distribution (see also Minniti et al. 2017; Prudil et al. 2019; Grady et al. 2020, for a discussion of the problem). To emphasize it again, unlike interstellar gas in the plane of the Galaxy, young and intermediate-age metal-rich stars (Binney et al. 1991; Babusiaux and Gilmore 2005; Bovy et al. 2019; Queiroz et al. 2021; Deka et al. 2022; Iwanek et al. 2023), these typically metal-poor stars do not trace a prominent bar. In addition, the impact of the bar's potential would expectedly be seen at lower Galactic latitudes, whereas our sample of objects is specifically at $|b|$ higher than 1.5° (see Sect. 2 below for an explanation).

In this connection, Molnar et al. (2022) recently published the VIrac VAriable Classification Ensemble (VIVACE) catalog, which features variable stars extracted from the Vista Variables in the Vía Láctea (VVV) variability survey with the advanced VISTA 4-m telescope in Paranal. The VVV Survey is an ESO public survey scanning the Galactic bulge and adjacent section of the southern mid-plane in the near-infrared (see Minniti et al. 2010; Saito et al. 2012; Surot et al. 2019, for details). Comparison with OGLE data obtained with the 1.3-m Warsaw telescope at the Las Campanas Observatory suggests completeness of the VIVACE-VVV catalog of around 90% for the fundamental-mode (or type-ab) RR Lyrae stars. As a demonstration of the potential of the catalog within the high extinction regions of the Galaxy, the spatial and kinematic properties of stars within the Galactic inner disk and bulge regions have been in outline studied. As a step forward, the aim of the present study is to draw upon the catalog to enhance the characterization of the bulge and relevant parameters associated with the Sun's position within the system under question. Actually, this paper is the closing of a series of publications with similar methods and goals but based on different data sets (Griv et al. 2020, 2021, 2022). In the series, we present the space distributions of sources with ages larger than (comparable to) 10 Gyr – RR Lyrae stars, Type II Cepheid stars, and globular clusters – occupying the almost nonrotating, that is to say, primarily pressure-supported bulge and halo in the Galaxy.

We will evaluate here the value of r_0 and make conclusions about the genesis of the bulge by using a contemporary sample of objects. Specifically, the spatial distribution of VIVACE RR Lyraes identified toward the central Galaxy will be rated using near-infrared photometry from the VVV survey. As a model of the bulge, an oblate spheroid of stars with two major perpendicular axes a (directed towards us) and b situated in the Galactic plane and a short axis c perpendicular to the plane is adopted. Comparing the new findings to existing determinations based on less extensive yet diverse samples of RR Lyraes, Type II Cepheids, and globular clusters is an ideal way to assess systematics. The VIVACE-VVV sample contains a total of 39,617 sources. The new results tied to deliberately chosen $\sim 20{,}000$ RR Lyraes are robust determinations including the Sun's distance from the GC and the density profile. Finally, we will make an examination and conclusion of all the work we have done in the series.

The study is divided as follows. In Sect. 2 the observational data are described. The results of model calculations are presented in Sect. 3. Our main consequences are summarised in Sect. 4. The selection of the observational material and the numerical method are briefly outlined in Appendixes A and B, respectively.

2 Observational data

The distance of a star from the GC is evidently

$$r^2 = (r_0 - d\cos b\cos l)^2 + d^2\cos^2 b\sin^2 l + (d\sin b + z_0)^2, \tag{1}$$

where $r_0 = 7.7 - 8.3$ kpc (Do et al. 2019; GRAVITY Collaboration 2019; Reid et al. 2019; VERA Collaboration 2020; Iwanek et al. 2023; Leung et al. 2023) and $z_0 = 10 - 25$ pc (Bland-Hawthorn and Gerhard 2016; Karim and Mamajek 2017; Bennett and Bovy 2019; Griv et al. 2021).

Figure 1 relays the spatial distribution of all $N_{\rm total} = 39{,}617$ RRab (Appendix A) in a Cartesian XYZ frame (the X-axis points to the GC, the Y-axis points to the direction of the Galactic rotation, and the Z-axis points to the North Galactic Pole). An axisymmetric distribution around the GC in the central part of the system is apparent. The sample stars fill mainly the bulge region between the Galactocentric distances ≈ 0.054 kpc and ≈ 4 kpc (assuming the location of

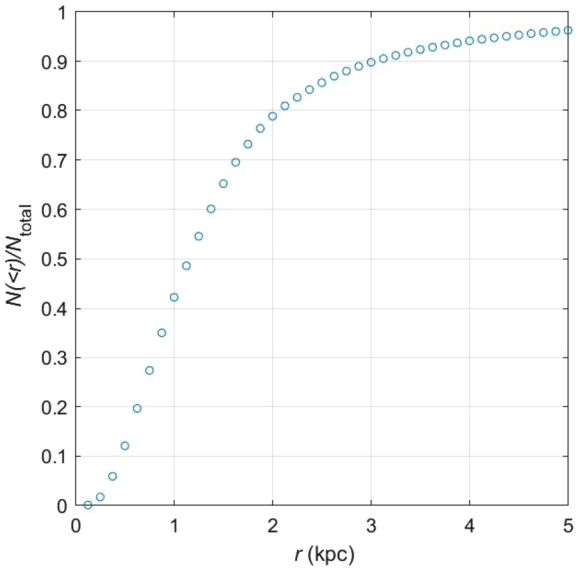

Fig. 2 Normalized cumulative distribution for all RRab

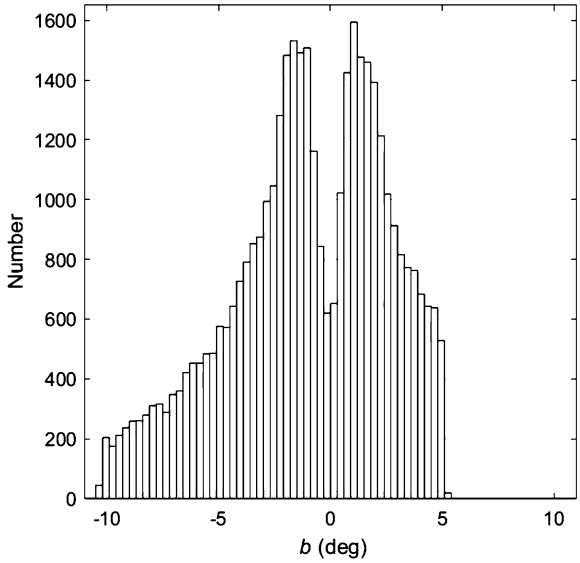

Fig. 3 Distributions of all RRab with respect to the Galactic latitude b

the Sun is $r_0 = 8.15$ and $z_0 = 15$ pc; equation (1)). The closest star to the GC is thus located at $r \approx 0.05$ kpc. Curiously, the closest candidate globular cluster to the GC is situated at a distance of about 0.4 kpc from the GC, that is, much farther away from the GC than RRab (Minniti et al. 2021). Note that the sample has stars beyond the bulge sampling the disk in the fourth Galactic quadrant.

The normalized distribution of all RRab is shown in Fig. 2. A convergence at $r = r_{\rm conv} \approx 3$ kpc is seen. The half-population radius for these objects is $r_{\rm hp} \approx 1$ kpc. Interestingly, the radius containing half of the Type II Cepheids population from the VVV survey by Braga et al. (2019) is also $r_{\rm hp} \approx 1$ kpc (Griv et al. 2021). In sum, the typically metal-poor RR Lyraes and Type II Cepheids are almost equally concentrated.

The distribution of all RRab with respect to b is shown in Fig. 3. It is important to notice that the stars of the sample cover almost all bulge areas, excluding the $|b| \lesssim 1.5°$ belt. As the extinction gets larger toward the Galactic mid-plane it forces the survey to its faint limit to pick up stars, and the uncertainties increase, and consequently, the probabilities in 'successful' classification schemes tend to decrease as a result. At $|b| \lesssim 1.5°$, extinction by interstellar dust concentrated mostly along the mid-plane draws the apparent magnitudes of sources beyond the faint detection limit of the VVV survey, causing the completeness of the sample to drop essentially (cf. Dékány et al. 2013; Griv et al. 2020; Pietrukowicz et al. 2020; Griv et al. 2021; Navarro et al. 2021). The VIVACE-VVV RR Lyrae stars observations at $|b| > 1.5°$ are, however, almost not affected by dust extinction. This is why only the high-latitude RRab attract our attention.

The cone-like volume with data in Fig. 1 is confined vertically to less than about 2.5 kpc near the GC. Therefore, increasing r to values $r > 2.5$ kpc does not increase the vertical range of data. As a consequence, the analysis is tied to high latitude ($|b| > 1.5°$) objects restricted within the bulge region, say, of $r = r_{\rm max} = 3.5$ kpc and the coordinate region given by equation (A.1), imposing a probability cutoff $p > 0.9$. We estimated that less than $\approx 10\%$ of stars are localized beyond $r_{\rm max} = 3.5$ kpc. The contribution of these distant objects to the likelihood function L (equation (B.4) in Appendix B) does not significantly impact the conclusions.

Figure 4 highlights a distribution of selected $N = 24{,}308$ RRab with respect to the l and b. The concentration of stars towards the GC is clearly seen. The figure conveys that the sample of objects populates nearly the entire axisymmetric bulge, excluding regions close to the GC and mid-plane.

The distributions of all and selected RRab with respect to distances d and r are shown in Fig. 5. As is apparent from Fig. 5, for two samples of stars – full and selected ones – the spatial distribution has approximately the same properties. The stars exhibit a centrally concentrated distribution towards the GC, and the spatial density of objects ρ in the range $1 < r < 6$ kpc can be described approximately by the standard power law with a constant flattening

$$\rho \propto r^{\alpha}, \tag{2}$$

where the power-law index $\alpha < 0$.

In the spirit of Harris (1996), Keller et al. (2008), and Mateu and Vivas (2018), we explore here the most basic model assuming that the spatial distribution of RRab is almost spherically symmetric (see Figs. 1 and 4), that is to say, $a = b \gtrsim c$ (see equations (B.1) and (B.3)). Sesar et al.

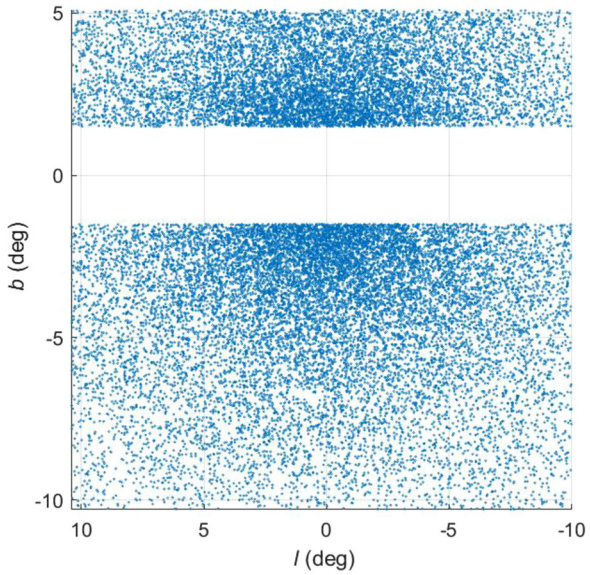

Fig. 4 Distribution of selected 24,308 RRab with respect to l and b

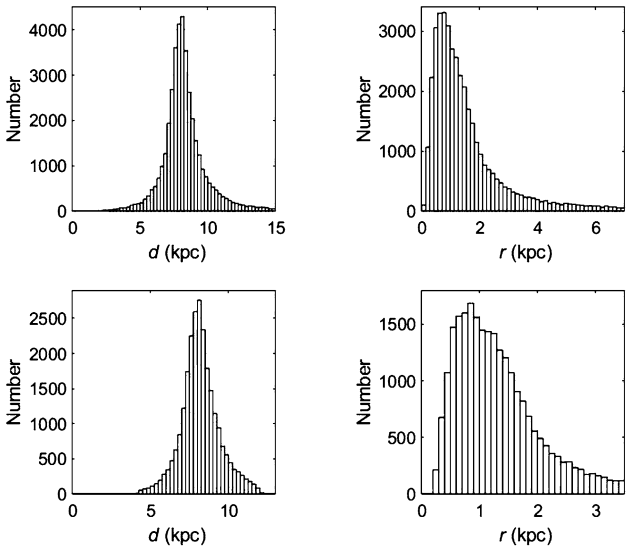

Fig. 5 Distribution of all RRab (upper panels) and selected RRab (bottom panels) with respect to distances d and r (assuming $r_0 = 8.15$ kpc and $z_0 = 0.015$ kpc)

(2013), Pietrukowicz et al. (2015), Hernitschek et al. (2019), Posti and Helmi (2019), and Navarro et al. (2021) have already used similar spheroidal models slightly flattened in the vertical direction (a model has $a = b$ and flattening described by the value of oblateness $q \equiv c/a \lesssim 1$).

3 Results of modeling

The parameters of a power-law density model are determined by a statistical method. The method of analysis (the modified Rastorguev et al. (1994) maximum likelihood method) is not significantly different from the previous work (Appendix B). For the uncertainties the effect of observational errors was taken into account. The results of distribution modeling of these stars for adopted bulge's radii $r_{\max}$ by using the method are given in Table 1.[3] As is seen, the main result – the value of the Sun's distance – changes slightly with variations of $r_{\max}$ in the range $1.5 - 3.5$ kpc. Moreover, changes in the value of the probability cutoff in the interval $0.85 < p < 0.95$ do not affect our main conclusions. We decided that approximately $r_0 = 8.1 \pm 0.1$ kpc, within $r_{\max} = 3.5$ kpc. Our *indirect* determination of r_0 of about 8.1 kpc is consistent with findings from Bland-Hawthorn and Gerhard (2016), Camarillo et al. (2018), Do et al. (2019), Reid et al. (2019), VERA Collaboration (2020), GRAVITY Collaboration (2021), Iwanek et al. (2023), and Leung et al. (2023). This distance is somewhat lower, but not significantly different, from values of $r_0 = 8.28 \pm 0.14$ kpc and $r_0 = 8.35 \pm 0.10$ kpc derived from the distributions of 16,221 OGLE RR Lyraes and 715 VVV Type II Cepheids in our previous works (Griv et al. 2020, 2021). Yet, the value of r_0 of about 8.1 kpc is notably lower than the 1986 IAU standard $r_0 = 8.5$ kpc (Kerr and Lynden-Bell 1986).

Thus, the r_0 values for fits with $r_{\max} = 1.5 - 3.5$ kpc are practically equal. But clearly in Table 1, the parameters α and q are sensitive to the choice of $r_{\max}$. The α and q values are varying systematically (and significantly!) with increasing $r_{\max}$. An increase of $|\alpha|$ from 1.56 to 2.66 and a decrease of q from 1.0 to 0.76 with the cut-off radius $r_{\max}$ is clearly seen. In conjunction with this, Navarro et al. (2021) have identified about 60 thousand type-ab RR Lyraes from the innermost regions of the Galaxy to the halo in the VVV, OGLE-IV, and *Gaia* DR2 catalogs and about 4 million red clump stars (RCs) in the 2MASS catalog.[4] The density distribution of RR Lyraes and RCs was fitted by three power laws over three radial intervals $r < 0.3$ kpc, $0.3 < r < 1.17$ kpc, and $1.17 < r < 4.8$ kpc and $r < 0.3$ kpc, $0.3 < r < 1.0$ kpc, and $1.0 < r < 4.8$ kpc (assuming $r_0 = 8.33$ kpc), respectively. An increase of $|\alpha|$ from 0.94 to 2.43 (for the sample of RR Lyraes) and from 0.64 to 3.41 (for the sample of RCs) with the cut-off radius $r_{\max}$ was already detected.

Remarkably, the average power-law index derived here from the VIVACE-VVV distribution of bulge stars, i.e. $< \alpha > \simeq -2.2$, is comparable to that inferred from the inner halo ($r < 25$ kpc) globular clusters of Baumgardt and Vasiliev (2021) investigated by Griv et al. (2022). Such a value of $< \alpha >$ is not too far from the value derived by Navarro et al. (2021) for the radial interval $1.17 < r < 4.8$

[3] As we found, the z_0 values for fits with $r_{\max} = 1.5 - 3.5$ kpc are about $0 - 2$ pc with substantial errors. It is impossible for that reason to understand which z_0 is correct. We adopted the constant value $z_0 = 0.015$ kpc in calculations (cf. Griv et al. 2022).

[4] RCs are low-mass, early K class red giants in the Hertzsprung-Russell diagram at around 5000 K in the stage of core helium-burning.

Table 1 The parameter set with maximum probability inferred from the VIVACE-VVV RRab of Molnar et al. (2022). Columns 1 to 5 highlight the following: the adopted cut in the data set $r_{\max}$, number of selected objects N inside $r_{\max}$ in the sample, Sun's distance r_0, power-law index α, and the oblateness $q = c/a$

$r_{\max}$ (kpc)	N	r_0 (kpc)	α	q
1.5	16,665	8.15 ± 0.05	-1.56 ± 0.02	1.0 ± 0.01
2.0	20,662	8.14 ± 0.04	-1.95 ± 0.02	0.99 ± 0.01
2.5	22,551	8.15 ± 0.04	-2.25 ± 0.03	0.96 ± 0.01
3.0	23,641	8.15 ± 0.03	-2.49 ± 0.03	0.85 ± 0.01
3.5	24,308	8.16 ± 0.04	-2.66 ± 0.03	0.76 ± 0.01

kpc. In the spirit of Alcock et al. (1998), the result derived here implies that the old bulge and inner halo form a continuous subsystem and the bulk of the bulge objects represents the inner extension of a centrally concentrated, almost axisymmetric halo in the Galaxy. This was already suggested in the previous papers of the series. The novel feature here is that it is confirmed in a truthful way by using a new, accurate sample of the bulge's stars. Such a hypothesis is consistent with a spherical-like bulge component originating from an early, ~ 10 Gyr ago, fast mass assembly, as suggested by numerous cosmological simulations (Brooks and Christensen 2016; Pérez-Villegas et al. 2017; Rojas-Arriagada et al. 2017; Rey et al. 2023). Kunder et al. (2020) and Pietrukowicz et al. (2020) have advanced a similar idea in interpreting the radial velocities of 2768 RR Lyraes toward the southern bulge and the photometric metallicities of almost 91,000 RR Lyraes toward the bulge and halo, respectively.

In the following, we use $r_{\max} = 2.5$ kpc for the cut in the data set (because here the volume containing more than 90% of the selected data is not much stretched along the line of sight; see Fig. 1). The Sun is therefore

$$r_0 = 8.15 \pm 0.04 \text{ kpc}$$

distant from the GC. The power-law index and the oblateness are

$$\alpha = -2.25 \pm 0.03$$

and

$$q = 0.96 \pm 0.01,$$

correspondingly. The distribution of selected RRab has the shape of an oblate spheroid with three axes of its symmetry of almost the same length. One concludes that the distribution of old stars within $r < 3$ kpc from the GC is spherical-like, $q \approx 1$.[5]

[5]In sharp contrast to our results, Pietrukowicz et al. (2015) have obtained a ratio of $a : b : c \approx 1 : 0.5 : 0.4$ by exploring RR Lyraes from the OGLE-III sample located only within the central ≈ 1 kpc.

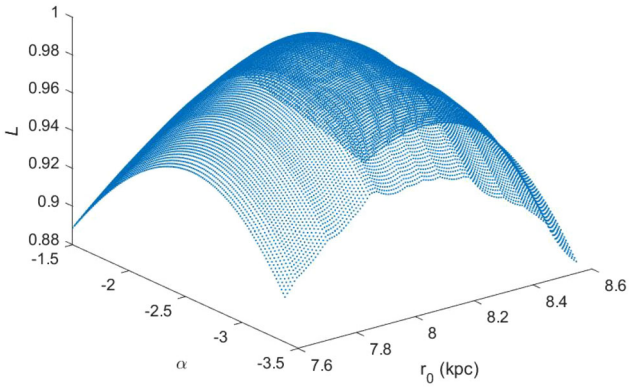

Fig. 6 The normalized likelihood L for selected 23,641 RRab of an original sample within $r_{\max} = 3$ kpc relative to parameters r_0 and α

It is important to note that our result of the Sun's distance is independent of the Do et al. (2019), Reid et al. (2019), VERA Collaboration (2020) as well as GRAVITY Collaboration (2021) direct estimates. As for us, making use of these $\sim 20{,}000$ stars with VIVACE-VVV photometric information leads to one of the most accurate indirect estimations of r_0 relying on the secondary calibration (i.e. a period-luminosity relationship).

In Fig. 6 the normalized likelihood is compared to r_0 and α for selected 23,641 stars of an original sample within the distance $r_{\max} = 3$ kpc (assuming $q = 1$). A well-defined maximum of L with respect to r_0 and α is clearly seen from the calculation, which backs a robust determination of the unknown quantities.

4 Summary

Our previous publications on the determination of morphology of the pressure-supported classical bulge in the Galaxy, composed primarily of Population II stars and globular clusters is revised. A maximum likelihood statistical method in the three-dimensional parameter space for stars is employed to derive r_0, α, and q of the bulge of the system by exploring $N \sim 20{,}000$ RRab identified in the recent Molnar

et al. (2022) VIVACE-VVV catalog. Their spatial distribution is approximated by a standard power law with a constant flattening and truncations at the lower $r_{\rm min} \approx 0.05$ kpc and upper $r_{\rm max} \approx 3.5$ kpc limits while allowing for the position of the Sun in the system, the power-law index, and the oblateness to be free parameters. The following results are obtained:

(i) The implied Sun's distance is almost the same for all $r_{\rm max}$ in the range $1.5 - 3.5$ kpc. The distance is $r_0 = 8.15 \pm 0.04$ kpc. Apparently, this value is one of the most accurate indirect, relying on the period-luminosity relationship estimations of r_0 as various classes of objects and wavelengths are used. This is a key result of the work. Yet, the value of $r_0 \approx 8.1$ kpc is notably lower than the 1986 IAU standard $r_0 = 8.5$ kpc. The finding is consistent with recent estimates ranging between $7.7 - 8.3$ kpc (Camarillo et al. 2018; Do et al. 2019; GRAVITY Collaboration 2019; Reid et al. 2019; VERA Collaboration 2020; Leung et al. 2023; Iwanek et al. 2023). The parameters α and q are, however, sensitive to the choice of $r_{\rm max}$.

(ii) Thus, the r_0 values for fits with $r_{\rm max} = 1.5 - 3.5$ kpc are almost equal, while the $|\alpha|$ and q values are varying systematically with increasing $r_{\rm max}$ in the ranges $1.56 - 2.66$ and $1.0 - 0.76$, correspondingly.

(iii) The distribution of old RRab within ≈ 3 kpc from the GC has the shape of an oblate spheroid with three perpendicular axes of its symmetry of almost the same length. The value of oblateness $q \approx 1$.

(iv) The average power-law indexes derived from the distribution of bulge RRab and inner halo globular clusters are fairly identical. This appropriate result demonstrates that the old bulge and inner halo form a continuous, undivided subsystem, and the bulk of the bulge ancient objects represents the inner extension of a centrally concentrated, almost axisymmetric halo in the system. The bulge extends, correspondingly, out to the inner halo. Such an idea is consistent with an old bulge component originating from an early, ~ 10 Gyr ago, fast mass assembly, as suggested by cosmological simulations.

(v) And, suitable changes in the truncation radius $r_{\rm max}$ and the probability cutoff p in the VIVACE classification scheme do not affect our main conclusions.

All in all, the data analyzed provides constraints on r_0, α, and q. The present communication discontinues a series on the distribution of objects in the old bulge of mostly ancient stars and globular clusters. The results cited here are generally consistent with our previous determinations (Griv et al. 2020, 2021, 2022). Extension of this work may be provided by studying the spatial distribution of VIVACE-VVV Type II Cepheids and globular cluster candidates (Palma et al. 2019; Obasi et al. 2021; Garro et al. 2022) identified toward the central Galaxy.

We take a weighted average and weighted uncertainty associated with all our indirect determinations of r_0 made in the series of four papers with appropriate observational data, and use that to argue that the ensuing result may be among the most robust estimates that exist, as certain of the findings are tied to optical passbands of OGLE RR Lyraes and globular clusters, and near-infrared passbands of VVV Type II Cepheids, VVV and VIVACE-VVV RR Lyraes. As a result, spatial distribution modeling of variable stars and globular clusters yields a mean of

$$r_0 = 8.2 \pm 0.1 \text{ kpc}.$$

In practice, such a value of the Sun's distance from the GC can be therefore finally advised.

In closing, an accurate determination of r_0 is hampered by countless second-order weak effects (see Majaess 2010, for a discussion). As an example, stars closer to the midplane may have nearer distances owing to blending and perhaps more spurious photometry. The latter implies that one will have a preferential sampling of stars on the near side of the bulge, rather than deeper in. Another bias that exists (there are many) is if there is indeed a bar-like or triaxial bulge distribution in the data, oriented at an angle $\theta \approx 20°$ along the Sun-GC line, with axis ratios $\approx 1 : 0.3 : 0.2$ and a scale-length of ≈ 1.5 kpc, and the near end of the bar pointing towards positive l (Babusiaux and Gilmore 2005; Wegg and Gerhard 2013; Pietrukowicz et al. 2015; Deka et al. 2022; Iwanek et al. 2023; Lucey et al. 2023). Then we preferentially sample those stars at positive l, i.e. closer. As well, the assumed form of the observed profile which is given by equation (2) is almost certainly inadequate for any class of tracers spanning the entire Galaxy, from the bulge to the halo. A much better model would be a broken power law with a sharp break at some variable radii (e.g. Navarro et al. 2021) or a smoothly varying power-law index, such as in the well-known Sérsic (1963), Einasto and Haud (1989), and Zhao (1996) models. An exponential profile for the bulge region would also naturally result in an increasing $|\alpha|$ (local logarithmic slope) with increasing $r_{\rm max}$ (Molnar et al. 2022, Fig. 20 therein) (cf. Table 1). For the bulge model, any density distribution with a maximum in the centre will lead to a similar L function shape with a well-defined maximum as shown in Fig. 6. The distance r_0 should be probably re-calculated for all possible density profiles (broken power-law, Sérsik, . . .). A posteriori comparison of the model with the data would be desired. Also, the uncertainty in the RRab period-luminosity relation and extinction coefficients might contribute to the uncertainty in the distance to the GC. Future studies can lend insights into the issues raised here.

Appendix A: Selection of the observational material

The VVV maps parts of the bulge and southern plane in five deep near-infrared passbands ($ZYJHK_{\rm s}$), where extinction

effects are lower than at optical wavelengths (e.g. Majaess et al. 2016). VVV observations foster the detection of RR Lyraes and Type II Cepheids point sources that would otherwise be obscured in the optical. The VVV bulge survey area covers ≈ 315 deg^2 within Galactic longitudes l and latitudes b (not to be confused with the axis b of the observed bulge's ellipsoid)

$$-10.0^\circ \leq l \leq +10.4^\circ \quad \text{and} \quad -10.3^\circ \leq b \leq +5.1^\circ. \quad \text{(A.1)}$$

Heliocentric distances d to a VIVACE sample of total $N_{\rm total} = 39{,}617$ type-ab RR Lyraes (RRab) were evaluated via Monte Carlo simulations following the approach adopted by Majaess et al. (2018). Specifically, the MK_s and $(J-K_s)_0$ functions inferred from LMC stars are $MK_s = (-2.66 \pm 0.06)\log P + (-1.03 \pm 0.06)$ and $(J-K_s)_0 = (0.31 \pm 0.04)\log P + (0.35 \pm 0.02)$. A LMC reddening and distance modulus of $E(B-V) = 0.13 \pm 0.02$ and $\mu_0 = 18.43 \pm 0.03$ were assumed (Majaess 2010; Majaess et al. 2011), in addition to a color-excess ratio and extinction law of $E(J-K_s)/E(B-V) = 0.48 \pm 0.01$ and $A_{K_s}/E(J-K_s) = 0.49 \pm 0.02$ (Majaess et al. 2016). Minniti et al. (2018) corroborated the extinction law adopted and obtained $A_{K_s}/E(J-K_s) = 0.484 \pm 0.040$.

Following Majaess (2010) and Majaess et al. (2018), we accept for individual statistical errors of d an average value equal to $\pm 4\%$. Notice the rather accurate stellar distances and the substantial number of objects in the sample. The distances were paired with l and b for all RRab exhibiting probabilities of $p > 0.85$ in the VIVACE classification scheme (see Molnar et al. 2022, for an explanation).

Appendix B: Numerical method

An ellipsoid of bulge objects with normalized perpendicular axes of symmetry a (and $a \equiv 1$) directed to the Sun and b in the Galactic plane and an axis c perpendicular to this plane is observed. Ellipsoidal isodensity contours for the system are expressed as

$$\frac{x^2}{a^2} + \frac{y^2}{b^2} + \frac{z^2}{c^2} = 1, \quad \text{(B.1)}$$

where $(x/a, y/b, z/c)$ are the Cartesian coordinates centred on the GC. The most general case of a triaxial ellipsoidal system $a \neq b \neq c$ is considered. The observed distribution function of N objects is simply

$$f(x_{\rm s}, y_{\rm s}, z_{\rm s}) = \mathcal{A}(r_0, \alpha, z_0, a, b, c) r^\alpha, \quad \text{(B.2)}$$

where $(x_{\rm s}, y_{\rm s}, z_{\rm s})$ are the coordinates of objects, $\mathcal{A}$ is the normalization factor, and the data points are independent of each other. In the case of ellipsoidal distribution of objects within the region $r_{\rm min} \leq r \leq r_{\rm max}$, the normalization factor is given by

$$\mathcal{A} = \frac{\alpha+3}{4\pi abc} \frac{1}{r_{\rm max}^{\alpha+3} - r_{\rm min}^{\alpha+3}}. \quad \text{(B.3)}$$

We write the likelihood function as

$$L(r_0, \ldots, c) = \prod_{i=1}^{N} f(r_i; r_0, \ldots, c), \quad \text{(B.4)}$$

and find numerically the six parameter values r_0, α, z_0, a, b, and c that maximize the likelihood. In the calculation, r_i and $\mathcal{A}$ were re-evaluated according to equations (1) and (B.3), respectively, for a given r_0 at each reference to equation (B.4). Each of the parameters of the system in our studies were estimated using the maximum likelihood method allowing other parameters to vary.

Acknowledgements The authors have benefited from productive discussions with their colleagues from the Department of Physics, at Ben-Gurion University and the Institute of Astronomy, at National Tsing-Hua University. One of us (E. G.) is grateful to Irena Zlatopolsky for her endorsement during the preparation of the paper. We thank the reviewer for providing several suggestions for improving the manuscript.

Author contributions E.G. and I.J. and Daniel Majaess wrote the main manuscript text and D.M. and D.M. submitted data. All authors reviewed the manuscript.

Funding The study was sponsored in part by the United States-Israel Binational Science Foundation, the Ministry of Immigrant Absorption, Israel in the framework of the program 'KAMEA', and the Israel Science Foundation. D. M. also acknowledges support from CNPq/Brazil through project-350104/2022-0. Dante Minniti gratefully acknowledges support from ANID BASAL projects ACE210002 and FB210003, from Fondecyt project 1220724, and from CNPq Brazil project 350104/2022-Q and I.-G. J. thanks to the Ministry of Science and Technology, Taiwan.

Data Availability The stellar data underlying this paper will be shared upon reasonable request to the corresponding author.

Declarations

Competing interests The authors declare no competing interests.

References

Alcock, C., et al.: Astrophys. J. **492**, 190 (1998)
Babusiaux, C., Gilmore, G.: Mon. Not. R. Astron. Soc. **358**, 1309 (2005)
Baumgardt, H., Vasiliev, E.: Mon. Not. R. Astron. Soc. **505**, 5957 (2021)
Bennett, M., Bovy, J.: Mon. Not. R. Astron. Soc. **482**, 1417 (2019)
Binney, J., Gerhard, O.E., Stark, A.A., Bally, J., Uchida, K.I.: Mon. Not. R. Astron. Soc. **252**, 210 (1991)
Bland-Hawthorn, J., Gerhard, O.: Annu. Rev. Astron. Astrophys. **54**, 529 (2016)

Bovy, J., Leung, H.W., Hunt, J.A.S., Mackereth, J.T., García-Hernández, D.A., Roman-Lopes, A.: Mon. Not. R. Astron. Soc. **490**, 4740 (2019)
Braga, V.F., et al.: A&A **625**, 151 (2019)
Brooks, A., Christensen, C.: In: Laurikainen, E., Peletier, R., Gadotti, D. (eds.) Galactic Bulges, p. 317. Springer, Heidelberg (2016)
Camarillo, T., Mathur, V., Mitchell, T., Ratra, B.: Publ. Astron. Soc. Pac. **130**, 24101 (2018)
Deka, M., Deb, S., Kurbah, K.: Mon. Not. R. Astron. Soc. **514**, 3984 (2022)
Dékány, I., Minniti, D., Catelan, M., Zoccali, M., Saito, R.K., Hempel, M., Gonzalez, O.A.: Astrophys. J. **776**, L19 (2013)
Do, T., et al.: Science **365**, 664 (2019)
Einasto, J., Haud, U.: A&A **223**, 89 (1989)
Garro, E.R., Minniti, D., Gómez, M., Fernández-Trincado, J.G., Alonso-García, J., Hempel, M., Zelada Bacigalupo, R.: A&A **662**, 95 (2022)
Genzel, R., Eisenhauer, F., Gillessen, S.: Rev. Mod. Phys. **32**, 3121 (2010)
Gonzalez, O.A., Gadotti, D.: In: Laurikainen, E., Peletier, R., Gadotti, D. (eds.) Galactic Bulges, p. 199. Springer, Heidelberg (2016)
Grady, J., Belokurov, V., Evans, N.W.: Mon. Not. R. Astron. Soc. **492**, 3128 (2020)
GRAVITY Collaboration (Abuter, R., et al.): A&A **625**, L10 (2019)
GRAVITY Collaboration (Abuter, R., et al.): A&A **647**, 59 (2021)
Griv, E., Gedalin, M., Pietrukowicz, P., Majaess, D., Jiang, I.-G.: Mon. Not. R. Astron. Soc. **499**, 1091 (2020)
Griv, E., Gedalin, M., Pietrukowicz, P., Majaess, D., Jiang, I.-G.: Mon. Not. R. Astron. Soc. **502**, 4194 (2021)
Griv, E., Gedalin, M., Jiang, I.-G.: New Astron. **93**, 101758 (2022)
Harris, W.E.: Astrophys. J. **81**, 1095 (1996)
Hernitschek, N., et al.: Astrophys. J. **871**, 49 (2019)
Iwanek, P., et al.: Astrophys. J. **264**, 20 (2023)
Karim, T., Mamajek, E.E.: Mon. Not. R. Astron. Soc. **465**, 472 (2017)
Keller, S.C., Murphy, S., Prior, S., DaCosta, G., Schmidt, B.: Astrophys. J. **678**, 851 (2008)
Kerr, F.J., Lynden-Bell, D.: Mon. Not. R. Astron. Soc. **221**, 1023 (1986)
Kormendy, J.: In: Laurikainen, E., Peletier, R., Gadotti, D. (eds.) Galactic Bulges, p. 431. Springer, Heidelberg (2016)
Kunder, A., et al.: Astrophys. J. **821**, L25 (2016)
Kunder, A., et al.: AJ **146**, 270 (2020)
Leung, H.W., Bovy, J., Mackereth, J.T., Hunt, J.A.C., Lane, R.R., Wilson, J.C.: Mon. Not. R. Astron. Soc. **519**, 948 (2023)
Liu, G., Huang, Y., Bird, S.A., Zhang, H., Wang, F., Tian, H.: Mon. Not. R. Astron. Soc. **517**, 2787 (2021)
Lucey, M., et al.: Mon. Not. R. Astron. Soc. **520**, 4779 (2023)
Majaess, D.J.: Acta Astron. **60**, 55 (2010)
Majaess, D.J., Turner, D.G., Lane, D.J., Krajci, T.: J. Am. Assoc. Var. Star Obs. **39**, 219 (2011)
Majaess, D., Turner, D., Dékány, I., Minniti, D., Gieren, W.: A&A **593**, 124 (2016)
Majaess, D., Dékány, I., Hajdu, G., Minniti, D., Turner, D., Gieren, W.: Astrophys. Space Sci. **363**, 127 (2018)
Mateu, C., Vivas, A.K.: Mon. Not. R. Astron. Soc. **479**, 211 (2018)
Medina, G.E., Hansen, C.J., Muñoz, R.R., Grebel, E.K., Vivas, A.K., Carlin, J.L., Martínez-Vázquez, C.E.: Mon. Not. R. Astron. Soc. **519**, 568 (2023)
Minniti, D., et al.: New Astron. **15**, 433 (2010)
Minniti, D., et al.: AJ **153**, 179 (2017)
Minniti, D., et al.: A&A **616**, 26 (2018)
Minniti, D., et al.: A&A **652**, 129 (2021)
Molnar, T.A., Sanders, J.L., Smith, L.C., Belokurov, V., Lucas, P., Minniti, D.: Mon. Not. R. Astron. Soc. **509**, 2566 (2022)
Navarro, M.G., Minniti, D., Capuzzo-Dolcetta, R., Alonso-García, J., Contreras Ramos, R., Majaess, D., Ripepi, V.: A&A **646**, 45 (2021)
Ness, M., Lang, D.: AJ **152**, 14 (2016)
Obasi, C., Gómez, M., Minniti, D., Alonso-García, J.: A&A **654**, 39 (2021)
Palma, T., et al.: Mon. Not. R. Astron. Soc. **487**, 3140 (2019)
Pérez-Villegas, A., Portail, M., Wegg, C., Gerhard, O.: Astrophys. J. **840**, L2 (2017)
Pietrukowicz, P., et al.: Astrophys. J. **811**, 113 (2015)
Pietrukowicz, P., et al.: Acta Astron. **70**, 121 (2020)
Posti, L., Helmi, A.: A&A **621**, 56 (2019)
Prudil, Z., Dékány, I., Catelan, M., Smolec, R., Grebel, E.K., Skarka, M.: Mon. Not. R. Astron. Soc. **484**, 4833 (2019)
Queiroz, A.B.A., et al.: A&A **656**, 156 (2021)
Rastorguev, A.S., Pavlovskaya, E.D., Durlevich, O.V., Filipova, A.A.: Astron. Lett. **20**, 591 (1994)
Reid, M.J.: Publ. Astron. Soc. Pac. **134**, 123001 (2022)
Reid, M.J., et al.: Astrophys. J. **885**, 131 (2019)
Rey, M.P., et al.: Mon. Not. R. Astron. Soc. **995**, 1012 (2023)
Rojas-Arriagada, A., et al.: A&A **601**, 140 (2017)
Saito, R.K., Zoccali, M., McWilliam, A., Minniti, D., Gonzalez, O.A., Hill, V.: AJ **142**, 76 (2011)
Saito, R.K., et al.: A&A **537**, 107 (2012)
Semczuk, M., Dehnen, W., Schönrich, R., Athanassoula, E.: Mon. Not. R. Astron. Soc. **509**, 4532 (2022)
Sérsic, J.L.: BAAA **6**, 41 (1963)
Sesar, B., et al.: AJ **146**, 21 (2013)
Simion, I.T., Belokurov, V., Irwin, M., Koposov, S.E., Gonzalez-Fernandez, C., Robin, A.C., Shen, J., Li, Z.-Y.: Mon. Not. R. Astron. Soc. **471**, 4323 (2017)
Surot, F., et al.: A&A **629**, 1 (2019)
Valenti, E., et al.: A&A **587**, L6 (2016)
VERA Collaboration (Hirota, T., et al.): Publ. Astron. Soc. Jpn. **72**, 50 (2020)
Wegg, C., Gerhard, O.: Mon. Not. R. Astron. Soc. **435**, 1874 (2013)
Yu, S.-Y., Xu, D., Ho, L.C., Wang, J., Kao, W.-B.: A&A **661**, 98 (2022)
Zhao, H.-S.: Mon. Not. R. Astron. Soc. **278**, 488 (1996)